Journal of Building Engineering 64 (2023) 105588

Contents lists available at ScienceDirect

Journal of Building Engineering

journal homepage: www.elsevier.com/locate/jobe

Effect of temperature rise inhibitor on early-age behavior and cracking resistance of high strength concrete under uniaxial restrained condition

Dejian Shen [a,b,c,*], Jiacheng Kang [a,b,c], Ci Liu [a,b,c], Ming Li [a,b,c], Yifan Wei [a,b,c,d], Liukun Zhou [a,b,c]

[a] College of Civil and Transportation Engineering, Hohai Univ., No. 1, Xikang Rd., Nanjing, 210024, China
[b] Jiangsu Engineering Research Center of Crack Control in Concrete, No. 1, Xikang Rd., Nanjing, 210024, China
[c] Nanjing Engineering Research Center for Prefabricated Construction, No. 1, Xikang Rd., Nanjing, 210024, China
[d] Nanjing Southern New Town Development & Construction (Group) Co.,Ltd, Daming Rd., Nanjing, 210022, China

ARTICLE INFO

Author keywords:
Early-age concrete
Temperature rise inhibitor
Cracking resistance
Tensile creep
Autogenous shrinkage

ABSTRACT

Temperature rise inhibitor (TRI) is used to modify the cement hydration and reduce the heat release of high strength concrete (HSC). Many investigations on the mechanical properties, temperature process, and autogenous shrinkage of cement-based materials with TRI have been conducted. However, the evaluation of the early-age behavior and cracking resistance of HSC with TRI under uniaxial restrained condition considering the effects of temperature, shrinkage, restrained stress, and tensile creep simultaneously was rarely conducted. Temperature stress test machine, which could measure these factors simultaneously, was used to investigate the effect of TRI contents on the early-age behavior and cracking resistance of HSC in this research. The peak temperature, temperature rising rate, autogenous shrinkage, and tensile creep decreased with increasing TRI contents. The addition of TRI improved the early-age cracking resistance of HSC. A modified stress-strain failure criterion and a prediction model for autogenous shrinkage of HSC with TRI were proposed.

1. Introduction

Although high strength concrete (HSC) has large annual consumption due to diverse sources, good durability, and relatively low cost, early-age cracking of HSC remains a problem in many practical engineering projects, e.g., urban rail transits, tunnels, high-rise buildings, and long-span bridges [1,2]. A site survey in 20 building city orbit traffic stations reveals that the cracking in the sidewall usually appears within 3–5 days, and 85.3% of leakage is caused by early-age cracking [3]. Cracks occur and develop quickly when the restrained stress of concrete induced by shrinkage deformation reaches its tensile capacity, which will destroy the integrity of the concrete structures. The aggressive substances can easily penetrate concrete through cracks, affecting the quality of concrete and causing many security problems [4–6]. The shrinkage deformation, which will increase the cracking risk of HSC, is related to many factors such as the chemical reaction of the materials, the temperature and humidity environment of concrete structures, and the restrained conditions [7]. Different kinds of shrinkage deformations occur in HSC at the early stage after pouring [8]. According to the difference in causes, the shrinkage deformation leading to non-load-related cracks can be divided into drying shrinkage, autogenous

* Corresponding author. College of Civil and Transportation Engineering, Hohai Univ., No. 1, Xikang Rd., Nanjing 210098, China.
E-mail address: shendjn@163.com (D. Shen).

https://doi.org/10.1016/j.jobe.2022.105588
Received 30 August 2022; Received in revised form 29 October 2022; Accepted 19 November 2022
Available online 26 November 2022

shrinkage (AS), thermal shrinkage, chemical shrinkage, carbonation shrinkage, and so on [9]. The early-age cracking of HSC is mainly caused by thermal shrinkage and AS [1,3]. HSC may have great self-desiccation and high temperature rise, and the peak temperature of HSC can reach around 70–80 °C. The volume of HSC changes greatly with changing temperatures, and restrained tensile stress develops when the temperature of HSC decreases gradually from the peak temperature, which will cause thermal cracking at early age. Besides, self-desiccation may lead to the development of AS. The restrained stress is higher in modern concrete structures with large volumes, large spans, and strong constraints than that in ordinary structures. Therefore, for the long-term sustainability of the HSC structures, investigating the methods to improve the early-age cracking resistance of HSC is of great importance.

To reduce the thermal shrinkage and improve the early-age cracking resistance of concrete, different methods such as compensating shrinkage, reducing hydration heat release, and improving the dissipation condition of heat have been proposed from the perspective of material [10]. Temperature rise inhibitor (TRI) is a polymeric admixture composed prepared by acid hydrolysis of corn starch to reduce the hydration heat release of concrete [11]. The addition of TRI would depress the main hydration peak to have a lower maximum heat flow and less heat release during the first few days, which may be beneficial in mitigating the delayed ettringite formation (DEF) risk. The difference in the heat flow is mainly caused by changing the C–S–H nucleation. Besides, the addition of TRI would mainly affect the C–S–H precipitation, and partly change the surface environment of the cement particle [2]. Many studies have been conducted on the properties of cement-based materials containing TRI, which mainly focus on the effect of TRI on cement hydration, mechanical properties, and AS of cement-based materials [1,3,10,12,13]. For instance, Zhang et al. [13] found that the addition of TRI delayed the growth of ettringite in pore solution and decreased the dissolution rate of aluminum from clinkers, which decreased the AS of cement paste. Li et al. [3] revealed that the concrete generated expansion deformation by adding a kind of TRI and slight expansion mixture (HME). Besides, with the addition of TRI, the cement hydration in the acceleration phase was reduced, and the main heat release peak was prolonged. The investigation on the effect of TRI (less than 0.15%) on cement hydration and heat evolution of cement pastes and mortars was conducted by Yan et al. [2], and the results showed that TRI had “depressing effect” on maximum heat flow, and “retarding effect” on heat release depending on the initial state. Wang et al. [14] reported that adding TRI (ranging from 0 to 1.5%) to mass concrete could reduce the maximum temperature rise, delay the arrival time of peak temperature, and improve the cracking resistance of that. However, the investigations on the early-age cracking resistance of HSC with TRI are still limited. Previous studies [15–17] have revealed that tensile creep (TC) plays a significant role in the evaluation of the early-age cracking resistance of HSC, which is important in reducing the stress induced by restrained thermal shrinkage and AS of HSC at early age. However, the investigation on the effect of TRI on TC of HSC at early age remains limited. Besides, the difference between the restrained conditions has a great effect on the TC of concrete. For instance, in the direct tensile test, the TC increases with increasing water-to-binder (w/b) ratios [18]. However, the TC of concrete under uniaxial restrained condition decreases with increasing w/b ratios at early age [5]. Thus, the investigation on the TC of concrete under uniaxial restrained condition is necessary. Considering that the TC of concrete under uniaxial restrained condition would be influenced by AS deformation, therefore, the characterization of TC and AS is important for evaluating the early-age cracking resistance of HSC with TRI under uniaxial restrained condition.

Temperature stress test machine (TSTM) test is an effective method considering several factors such as temperature, shrinkage, restrained stress, and creep, to evaluate the early-age cracking resistance of HSC under uniaxial restrained condition [5,19,20]. TC, AS, restrained stress, and temperature process of concrete can be obtained through TSTM test simultaneously based on the results obtained by free and restrained specimens [19,21]. The representative volume element in mass concrete is treated as a specimen in the sealed condition, and the simulation of internal condition in mass concrete can be conducted by TSTM test with the temperature controlling molds by providing a nearly adiabatic condition [22]. Thus, using TSTM to evaluate the early-age cracking resistance of HSC with TRI could simultaneously consider the effects of TC, AS, restrained stress, and temperature process, which is of great significance to the investigation on the effect of TRI on the cracking resistance of HSC at early age.

Many criteria based on the TSTM test are proposed to evaluate the early-age cracking resistance of concrete, e.g., cracking stress [23], cracking temperature [24], cracking age [25], ratio of cracking stress to tensile strength [26], and stress reserve [27]. The difference between the cracking resistance of different concrete mixtures could be evaluated by these criteria, however, the cracking resistance of a single concrete mixture fails to be evaluated. Thus, proposing a criterion for evaluating the cracking resistance of a single concrete mixture is necessary.

Table 1
The chemical and physical properties of Portland cement.

Item	Portland cement
SiO_2	19.9%
Al_2O_3	4.6%
Fe_2O_3	3.0%
CaO	64.6%
MgO	0.78%
SO_3	2.37%
Na_2O	0.06%
K_2O	0.65%
Specific surface area	375 m^2/kg
3-d compressive strength	35.6 MPa
28-d compressive strength	66.9 MPa
Initial setting time	159 min
Final setting time	213 min

In this research, the effect of TRI on the cracking resistance of HSC at early age was investigated. The mechanical properties, temperature process, AS, restrained stress, and TC of HSC containing different TRI contents (0, 0.5%, 1.0%, and 1.5% by weight of cement power) were tested. A modified stress-strain failure criterion and a prediction model for AS of HSC with TRI were proposed.

2. Experimental work

The initial and final setting time, slump, compressive strength, splitting tensile strength, and elastic modulus at different ages were tested for HSC with different TRI contents. The TSTM tests were conducted to investigate the effect of TRI content on the early-age TC and cracking resistance of HSC.

2.1. Materials and mixture proportions

Portland cement (P·II 52.5R) was utilized according to the Chinese Standard GB 175 [28] and ASTM C150 [29]. Table 1 depicts the chemical and physical properties of Portland cement. Crushed limestone with a maximum aggregate size of 20 mm, and natural river sand with a fineness modulus of 2.33 were used as coarse and fine aggregate, respectively. Fig. 1 depicts the aggregate size grading curves obtained as a result of the sieve analysis. A polycarboxylate-based superplasticizer was taken to adjust workability.

A kind of starch-based TRI was used. The photograph of TRI and the molecular structure of starch are depicted in Fig. 2. Table 2 shows the basic properties of TRI.

The w/b ratio of the samples was constant at 0.32 in this research. The TRI content was 0, 0.5%, 1.0%, and 1.5% by weight of cement, as recommended in [14]. Table 3 depicts the mixture proportions of the specimens. TRI00 represents the reference concrete without TRI content. TRI05, TRI10, and TRI15 represent HSC incorporated with 0.5%, 1.0%, and 1.5% TRI contents.

In the specimen preparation, all the dry materials (i.e., coarse aggregate, fine aggregate, cement, and TRI) were added to the mixer and mixed for 3 min ensuring that the ingredients were uniform. After that, tap water together with the superplasticizer was added to the mixer slowly. The mixtures were mixed for another 3 min finally.

2.2. Setting time, slump, and mechanical properties tests

The initial and final setting times of fresh pastes were tested using the Vicat apparatus according to ASTM C191 [30]. The slump of the fresh concrete was measured using the standard slump test apparatus according to ASTM C143 [31]. Compressive strength, splitting tensile strength, and elastic modulus were tested according to Chinese Standard GT/B 50081 [32]. Three cubic samples of size 150 mm × 150 mm × 150 mm were used for TRI00, TRI05, TRI10, and TRI15 concretes in the compressive strength and splitting tensile strength test. Three prismatic samples of size 150 mm × 150 mm × 300 mm were used for the elastic modulus test. The results of mechanical properties were calculated by the average values of three samples. After the samples were cast for 24 h, the samples were cured at a constant temperature of $20 \pm 1\ ^{\circ}C$ and relative humidity of 95 ± 2 %. The mechanical properties tests were conducted by Electro-hydraulic Servo Universal Testing Machine at 1, 3, 7, and 28 d.

2.3. TSTM test

2.3.1. Curing mode for TSTM test

Considering that the interior of mass concrete is insulated well, it takes a long time for the temperature to drop to ambient temperature [33,34]. The temperature history of mass concrete is close to semi-adiabatic curing mode, thus the semi-adiabatic curing mode was employed on TRI00, TRI05, TRI10, and TRI15 concretes to simulate the temperature history inside the mass concrete.

The temperature of the samples developed freely due to the hydration process, and the temperature was maintained for 36 h after reaching the peak temperature. Then, the temperature was cooled down at a rate of 1 °C/h until the samples cracked.

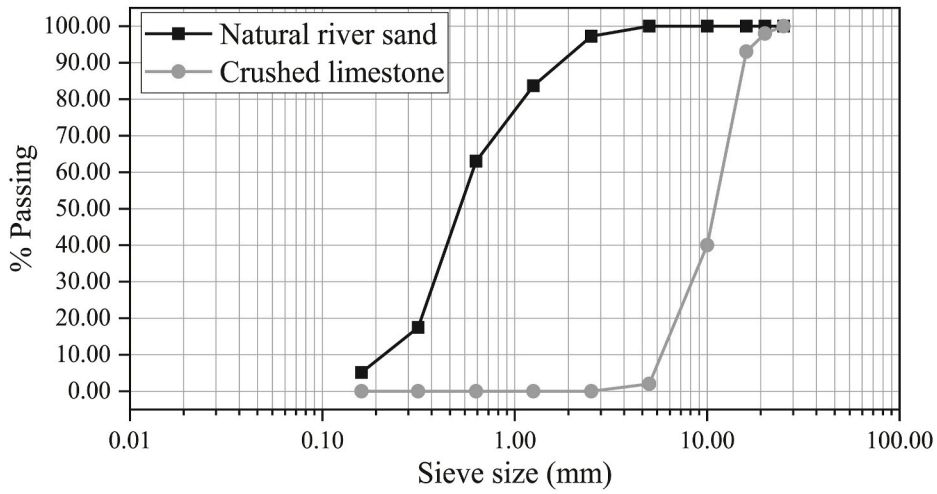

Fig. 1. Aggregate size grading curves.

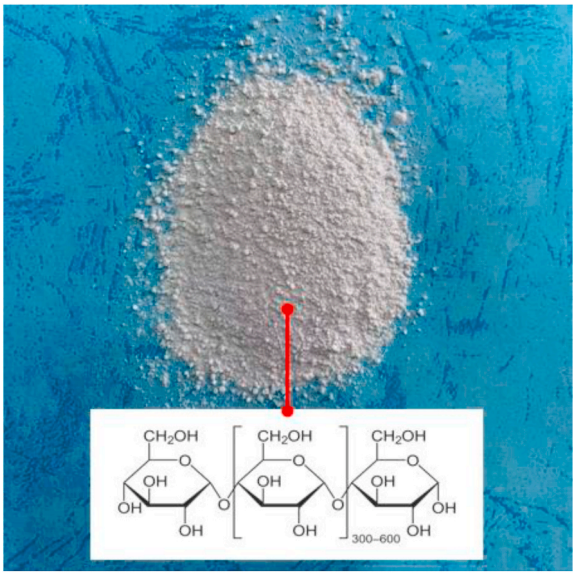

Fig. 2. Photograph of temperature rise inhibitor and the molecular structure of starch.

Table 2
Basic properties of temperature rise inhibitor [2].

Admixture	SSA(m^2/g)	Solubility at 20 °C	Alkaline stability	Peak molecular weight (Mw)	PDI
TRI	0.49	Low	Good	4957	1.368

[a]PDI (Polymer dispersity index) = Mw/Mn, Mn stands for mean molecular weight.

Table 3
Mixture proportions.

Concrete mix	Mixture parameters		Amount of materials (kg/m^3)					
	w/b	TRI(%)	Cement	TRI	Fine aggregate	Coarse aggregate	Water	Superplasticizer
TRI00	0.32	0	460	0	680	1120	147.2	3.68
TRI05	0.32	0.5	460	2.3	680	1120	147.2	3.68
TRI10	0.32	1	460	4.6	680	1120	147.2	3.68
TRI15	0.32	1.5	460	6.9	680	1120	147.2	3.68

2.3.2. Testing equipment

The TSTM mainly consisted of two dog bone-shaped molds, a temperature controlling system, displacement measurement system, load recording system, and a stepper motor, as depicted in Fig. 3. Two molds were identical in dimension, and were utilized for free shrinkage deformation as well as restrained shrinkage deformation measurement. The dimension of the center part of molds was 150 mm × 150 mm × 1500 mm, and both ends of the molds were in the dimension of 150 mm × 280 mm × 160 mm. A displacement sensor was mounted on the straight part of specimens to record deformation. The gripped end of the restrained shrinkage specimen was connected to the stepper motor. In this research, when the incremental deformation of the restrained specimen approached 2 μm, the restrained shrinkage specimen was pulled or pushed to the original position through the stepper motor to ensure that the specimen was under full restrained condition [35,36]. Restrained stress in the restrained shrinkage specimen was recorded with a load cell. The temperature of concrete was recorded with a temperature sensor, and the temperature process of the concrete specimen was controlled by a heating-cooling system with circulating liquid in the outer part of the mold. The temperature sensor was inserted into the concrete through the hole reserved in the cover of mold to record the temperature in the middle of the concrete. More details of TSTM can be found elsewhere [37].

2.3.3. Testing procedure

The fresh concrete was poured into the molds directly, and a plastic film sheet was placed in the mold before pouring to reduce friction between the mold and the concrete specimen, as recommended in [38]. The concrete specimens were sealed immediately to reduce moisture evaporation. The temperature sensor was inserted in the central part of the concrete specimen directly after pouring. Concrete specimens were cured and tested under the same curing condition for a single experiment. The two concrete specimens were covered around by the temperature-regulation molds, which included circulating fluid flowing in the pipes, to ensure the uniform

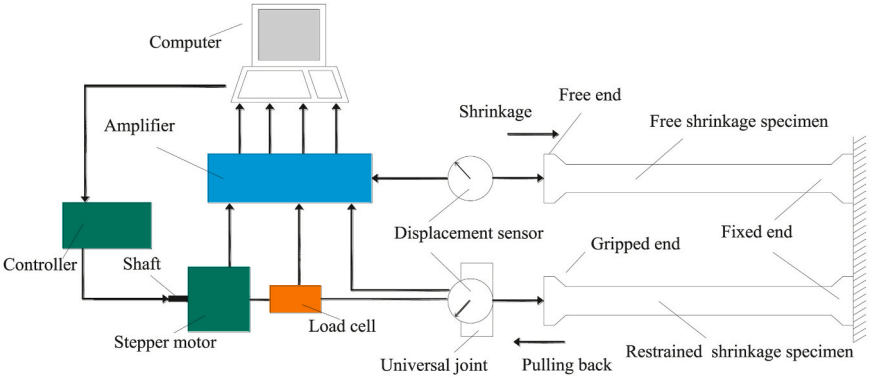

(a) Schematic diagram of TSTM [39]

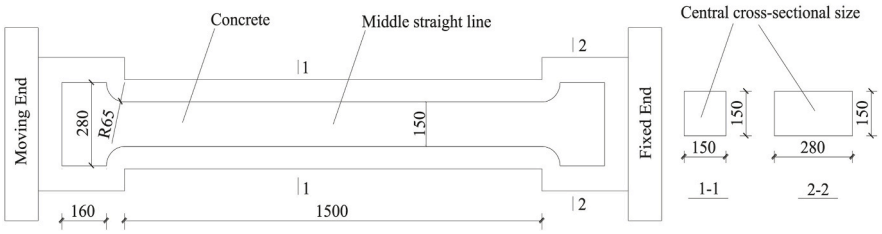

(b) Schematic diagram of specimen mold (mm)

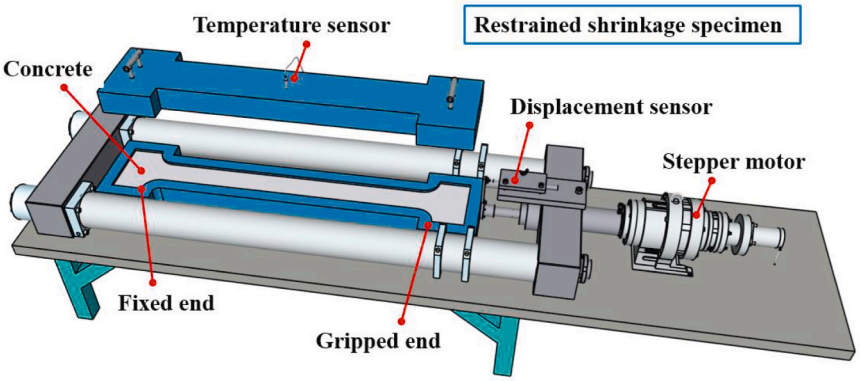

(c) Schematic diagram of restrained shrinkage specimen

Fig. 3. Schematic diagrams of TSTM.

temperature distribution over the cross section and to ensure the two concrete specimens had the same temperature history, as recommended in [39,40]. The temperature change inside the restrained shrinkage specimen was measured by the temperature sensor, and then the temperature of circulating fluid flowing in the mold pipes was adjusted to the same temperature as the internal temperature of the restrained shrinkage specimen. The temperature of the two concrete specimens was then adjusted so that the temperature of both specimens was always the same as the temperature of the core of the restrained shrinkage specimen. Due to the small cross sectional dimensions, the specimens were found to have a quite uniform temperature distribution at all times. The results of

Table 4
Slump and setting time of fresh concretes.

Concrete	Setting time (h)		Slump (mm)
	Initial	Final	
TRI00	4.75	12.50	130
TRI05	5.50	14.50	128
TRI10	6.00	24.50	127
TRI15	14.50	26.50	126

temperature, restrained stress, and deformation of the specimen were automatically recorded by a computer. Measurements started after pouring, and the data were recorded every 5 min.

3. Results and discussion

3.1. Slump, setting time, and mechanical properties of HSC with TRI

Table 4 lists the characteristics of fresh mixes. It could be observed that the initial and final setting times of specimens were delayed with increasing TRI contents. The initial setting time or final setting time of fresh mixes increased by 15.8%, 26.3%, and 205.3%, or 16.0%, 96.0%, and 112.0% with increasing TRI contents ranging from 0 to 0.5%, 1.0%, and 1.5%, respectively.

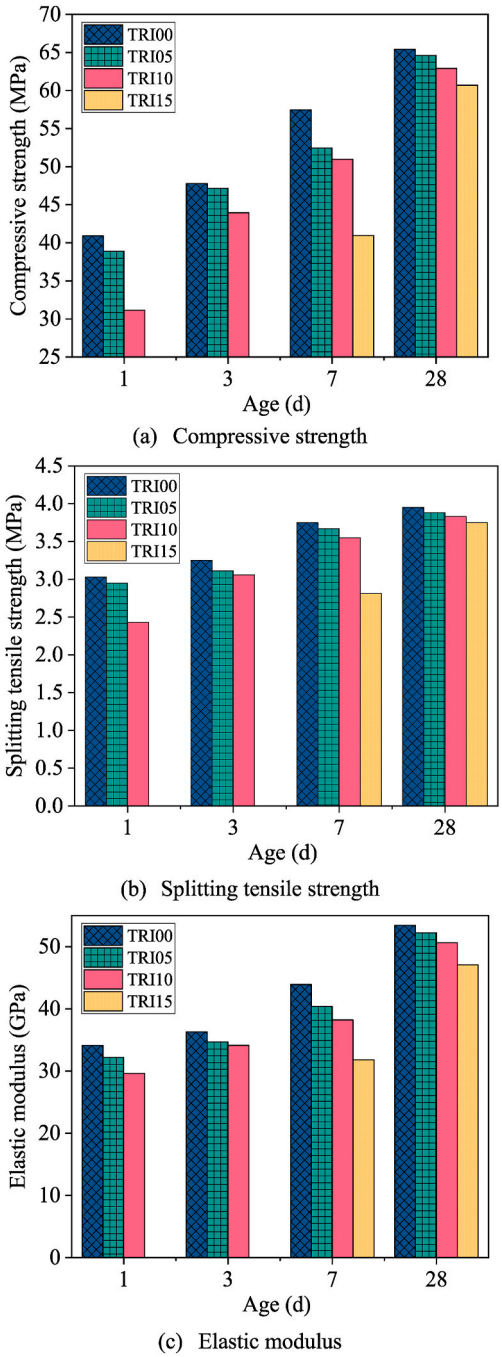

Fig. 4. Mechanical properties of hardened HSC for four specimens.

Fig. 4 depicts the characteristics of hardened HSC, and the results represent the average value of three samples. The results of TRI15 at 1 and 3 d were not tested due to the final setting time of that was very late, and the results were almost zero. The compressive strength decreased with increasing TRI contents, and the gap between HSC with different TRI contents decreased with age and was small at 28 d, as depicted in Fig. 4(a). The 28-d compressive strength of TRI00, TRI05, TRI10, and TRI15 concretes was 65.40, 64.62, 62.91, and 60.70 MPa, respectively. The 1-d or 28-d compressive strength decreased by 1.19%, 3.81%, and 7.19% with increasing TRI contents ranging from 0 to 0.5%, 1.0%, and 1.5%, respectively. The evolutions of splitting tensile strength of HSC with different TRI contents are depicted in Fig. 4(b). The effect of TRI content on variation tendencies of splitting tensile strength was consistent with that of compressive strength due to the analogous influence mechanism. The 28-d splitting tensile strength of TRI00, TRI05, TRI10, and TRI15 concretes was 3.95, 3.88, 3.83, and 3.75 MPa, respectively. The 28-d splitting tensile strength decreased by 1.77%, 3.04%, and 5.06% with increasing TRI contents ranging from 0 to 0.5%, 1.0%, and 1.5%, respectively. The compressive and splitting tensile strength of HSC with TRI was lower than that of TRI00 concrete, however, both of them reached 90% of that of TRI00 concrete at 28 d. This result may be explained by the fact that the growth and nucleation of C–S–H at early age are hindered by adding TRI. However, the hydration degree of cement is not affected by that at a later age [11].

As depicted in Fig. 4(c), the elastic modulus decreased with increasing TRI contents, and the gap between HSC with different TRI contents was small at 28 d. The 28-d elastic modulus of TRI00, TRI05, TRI10, and TRI15 concretes was 53.45, 52.23, 50.65, and 47.06 GPa, respectively. The 28-d elastic modulus decreased by 2.28%, 5.24%, and 11.96% with increasing TRI contents ranging from 0 to 0.5%, 1.0%, and 1.5%, respectively. The reason for the change of elastic modulus was similar to that for the strength. The hydration of HSC with TRI was hindered seriously, and more TRI contents led to a slower elastic modulus development.

3.2. Results of TSTM test

The temperature process, total deformation strain, and restrained stress were measured by the TSTM system. The total deformation strain was measured from the free shrinkage specimen, and the restrained stress was measured from the restrained shrinkage specimen. The two specimens of the same concrete were cured under the same temperature process.

The temperature process of four specimens measured by TSTM is depicted in Fig. 5. The pouring temperature or peak temperature of TRI00, TRI05, TRI10, and TRI15 concretes was 24.34, 19.16, 21.62, and 18.98 °C or 65.57, 59.42, 55.20, and 45.19 °C, respectively. The TRI00, TRI05, TRI10, and TRI15 concretes reached peak temperature at 30.5, 35.5, 47.5, and 119.5 h, respectively. The peak temperature of concrete decreased obviously with increasing TRI contents, and the temperature rising rate was reduced by adding TRI. The temperature rise of concrete was defined as the difference between the peak temperature and pouring temperature. The value of temperature rise was 41.23, 40.26, 33.58, and 26.21 °C for TRI00, TRI05, TRI10, and TRI15 concretes, which decreased by 2.35%, 18.55%, and 36.43% with increasing TRI contents ranging from 0 to 0.5%, 1.0%, and 1.5%, respectively. In addition, when the TRI content was 1.5%, the temperature rising stage of concrete was delayed by around 60 h, a similar phenomenon was also found in the setting time test, as depicted in Table 4. There are several possible explanations for this result. Firstly, the addition of TRI inhibits the nucleation of C–S–H and the hydration of C_3S [2], which reduces the initial hydration release rate of cement. The induction period would be prolonged lightly when the contents of TRI are small. When the content of TRI was 1.5%, the induction period was prolonged seriously in this research. Secondly, the peak temperature occurs when most of the surface of all generations is covered by C–S–H needles [2]. The addition of TRI suppresses the nucleation of C–S–H continuously, which makes the surface coverage low during the acceleration period. Thus, the peak temperature decreased with increasing TRI contents. Zhang et al. [1] reported similar results that the addition of TRI caused a large change in the rate and the extent of cement hydration. The maximum heat flow decreased with increasing TRI contents ranging from 0.2% of a mass fraction to 0.6%. Besides, TRI decreased the rate of heat release during the

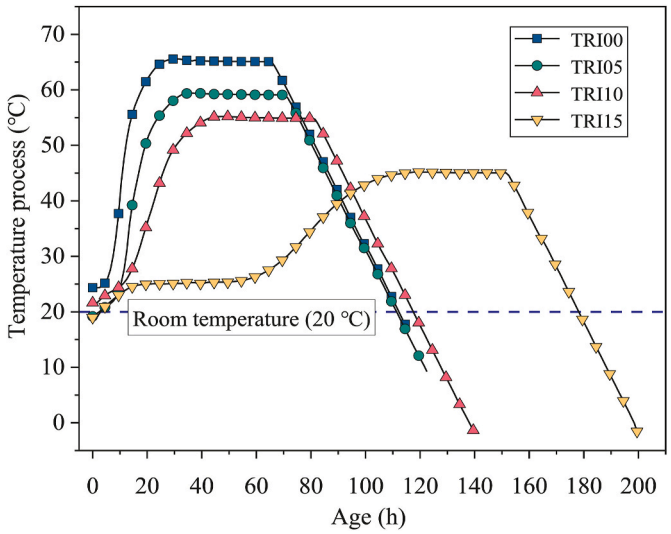

Fig. 5. Temperature process of four specimens.

acceleration period of the cement hydration process.

Fig. 6 depicts the total deformation of the free shrinkage specimen. It is worth noting that the HSC with different TRI contents had two peak expansion deformations. Four specimens all expanded initially, however, the addition of TRI caused different degrees of shrinkage, which caused the first peak expansion for HSC with different TRI contents. The shrinkage of HSC increased with increasing TRI contents at this stage. Then, the total deformation of four specimens expanded again as the temperature rose rapidly due to the hydration of cement. The second peak expansion strain after the temperature rising period was 186, 118, 112, and −7 με for TRI00, TRI05, TRI10, and TRI15 concretes, which decreased by 36.56%, 39.78%, and 103.76% with increasing TRI contents ranging from 0 to 0.5%, 1.0%, and 1.5%, respectively. When the content of TRI was 1.5%, although the hydration of cement after the first peak expansion occurred caused expansion of the specimen, the total deformation of concrete was in the state of contraction due to the large shrinkage deformation at a very early stage. The HSC specimens began to shrink as HSC entered the cooling period.

The results of restrained stress of restrained shrinkage specimen are depicted in Fig. 7. When the contents of TRI ranged from 0 to 0.5%, and 1.0%, the HSC specimens were subjected to compressive stress with a maximum value of 1.72 (at 23.5 h), 0.80 (at 31.5 h), and 0.61 MPa (at 44.5 h), respectively. The restrained stress of TRI15 concrete was almost zero during the temperature rising period. The restrained compressive stress decreased with increasing TRI contents, which attributed to lower temperature rise and thermal expansion of HSC under restrained condition. During the cooling period, the restrained tensile stress of four specimens developed rapidly and almost at the same rate. The cracking stress was 1.90, 1.95, 2.11, and 2.21 MPa for TRI00, TRI05, TRI10, and TRI15 concretes, which increased by 2.63%, 11.05%, and 16.32% with increasing TRI contents ranging from 0 to 0.5%, 1.0%, and 1.5%, respectively. TRI00, TRI05, and TRI10 reached peak temperature at 30.5, 35.5, and 47.5 h, respectively. It could be found that the occurrence time of maximum compressive stress was a little earlier than that of peak temperature. A similar phenomenon can be found in the studies [40,41]. A possible explanation for this might be that during the temperature rising period, the magnitude of restrained stress of concrete is mainly determined by a combination of compressive stress caused by temperature rise, tensile stress caused by AS deformation, and stress relaxation. Firstly, when the temperature of concrete approaches the peak temperature, the development of compressive stress caused by temperature rise gradually slows down. This phenomenon is mainly due to two reasons, one is the slowdown of the temperature rise rate and the other is the gradual reduction of coefficient of thermal expansion (CTE) to a relatively stable value at this time. Secondly, when the temperature of concrete approaches the peak temperature, the AS of concrete develops more quickly. Thirdly, stress relaxation occurs when the concrete is under restrained condition at early age. Therefore, the maximum compressive stress of concrete occurred a little earlier than that of peak temperature. After entering the constant temperature curing period, the compress stress of concrete decreased gradually partly due to the presence of stress relaxation.

Fig. 8 depicts the deformation strain of restrained shrinkage specimens for four specimens. When the incremental deformation of the restrained specimen approached 2 μm (1.3 με), the restrained shrinkage specimen was pulled or pushed to its original position, and restrained stress was recorded. The restrained stress depicted in Fig. 7 was a cumulative value. At the early stage of HSC after pouring, the specimens expanded initially, and were pushed back to the original position, thus causing the restrained compressive stress to increase. The times that TRI15 concrete was pulled back to the original position were significantly fewer than other HSC specimens with less TRI contents, and the elastic modulus of TRI15 concrete was low at this stage, thus the restrained stress was almost zero before the cooling point.

3.3. Early-age AS of HSC with TRI

Considering that the stiffness of fresh concrete was weak and no stress was generated in the TSTM test, the value of AS was set to be zero before the point of time-zero, as recommended in [42–44]. The definitions of time-zero are different in studies [43–52], such as setting time, onset of internal relative humidity drop, onset of capillary pressure, transition point from the autogenous strain curve, and the moment when the restrained stress occurred. Considering that only stress-induced deformation was analyzed in this research, the

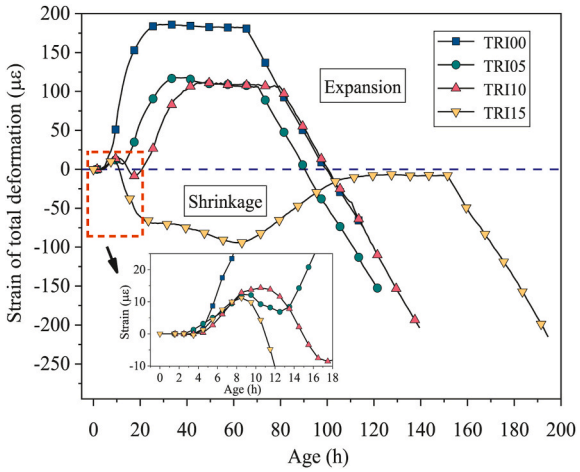

Fig. 6. Total deformation of free shrinkage specimen.

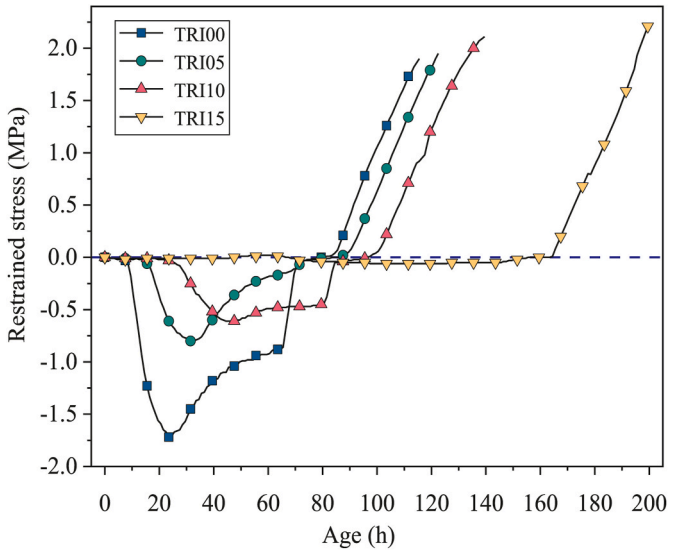

Fig. 7. Restrained stress of restrained shrinkage specimen.

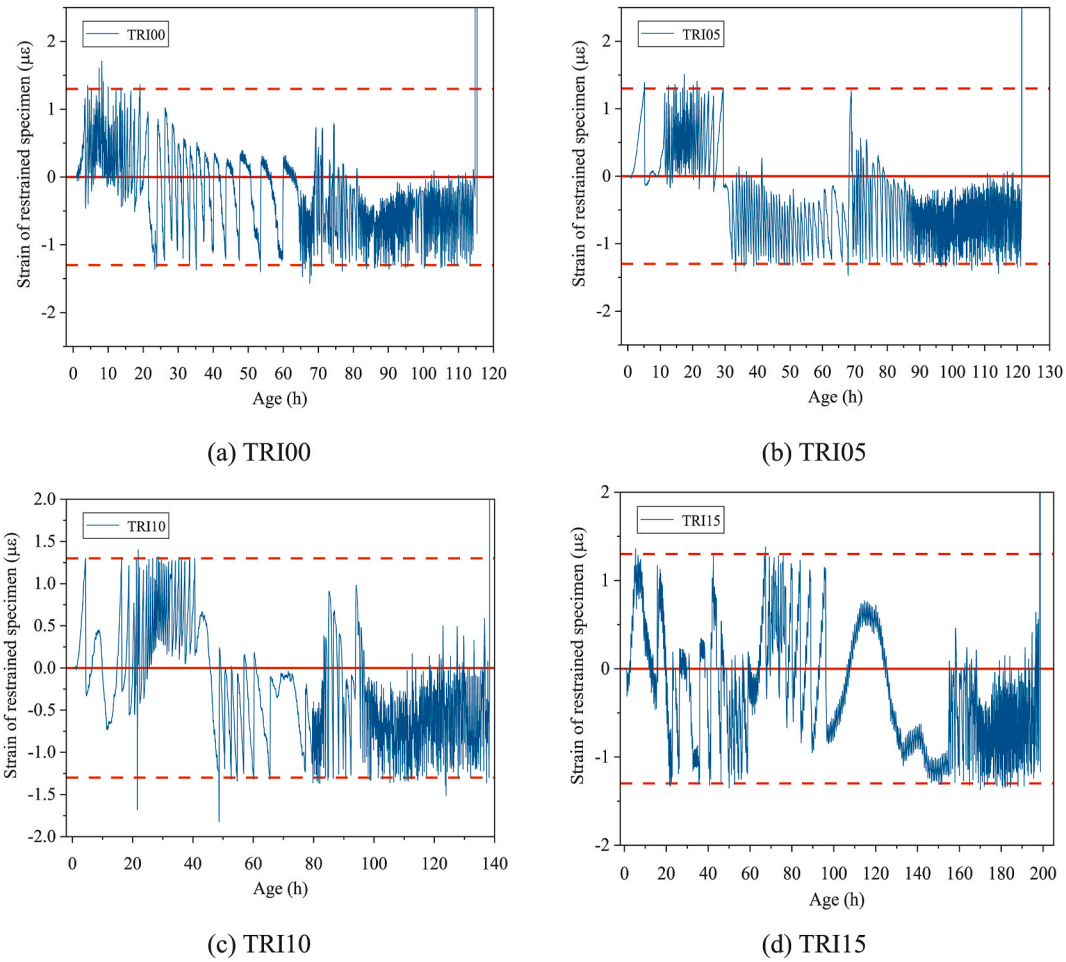

Fig. 8. Deformation strain of restrained specimens.

moment when the restrained stress occurred was taken as the time-zero of deformation, as recommended in [6,44], and the restrained stress could be recorded by the load cell.

AS is defined as the shrinkage without volume change caused by the loss or ingress of substances, temperature, external force, and restrained conditions [9]. The variation of the total deformation, the AS, and the thermal deformation is given in Eq. (1) [53].

$$\Delta\varepsilon_{tf} = \Delta\varepsilon_{as} + \alpha \times \Delta T \tag{1}$$

in which $\Delta\varepsilon_{tf}$ = total deformation of free shrinkage specimen, in με; $\Delta\varepsilon_{as}$ = AS deformation, in με; α = CTE, in με/°C; and ΔT = temperature change, in °C.

Generally, the value of CTE is set as constant in the calculation of thermally induced deformation, which will introduce an inaccuracy to the determination of AS [54]. However, the value of CTE changes with time and moisture content for hardening concrete [55]. Hence, to better predict the CTE and evaluate the AS in this research, the value of CTE was determined by Eq. (2), which was a modified prediction model for CTE changing with time. The same prediction model for CTE can also be found in studies [56–58].

$$\alpha_T(t) = \alpha_k \times [1 + 41 \times (t \cdot 24)^{-m}] \tag{2}$$

in which $\alpha_T(t)$ = time-dependent CTE, in με/°C; t = age of concrete after pouring, in d; α_k = average value of CTE during the cooling period, in με/°C; and m = an empirical parameter related to cement type and mineral admixture (value = 2.0).

The most early-age AS occurred during the temperature rising period and constant temperature curing period. Therefore, in the cooling period, most of the deformation was caused by the temperature change, and the CTE of concrete decreased to a constant value within 1 day, as reported in [59]. Therefore, the average CTE of concrete in the cooling period could be considered as the CTE of concrete at the age of 28 days of concrete and calculated by dividing the deformation change by the temperature change. In this research, the average value of CTE during the cooling period was calculated by Eq. (3).

$$\alpha_k = \frac{\Delta\varepsilon}{\Delta T} = \frac{\varepsilon_{cr} - \varepsilon_{co}}{T_{cr} - T_{co}} \tag{3}$$

in which ε_{cr} = strain of free shrinkage specimen at cracking age, in με; ε_{co} = strain of free shrinkage specimen at the starting point of the cooling period, in με; T_{cr} = temperature of free shrinkage specimen at cracking age, in °C; and T_{co} = temperature of free shrinkage specimen at the starting point of cooling period, in °C. The results of the average value of CTE during the cooling period were 5.09, 5.21, 5.38, and 5.03 με/°C for TRI00, TRI05, TRI10, and TRI15 concretes, respectively. The CTE was also tested using TSTM in the study [60], and the results revealed that the CTE of concrete was around 20–30 με/°C at the early stage of hardening, with the development of age, the value of CTE decreased gradually to a stable value ranging from 4.6 to 10.0 με/°C. The range of CTE values for different concretes reflects the variation in CTE of concrete's component materials. The aggregate type has the greatest effect on the CTE of concrete [61]. In this research, the w/b ratio, the amount of aggregates, and the amount of cement were constant for four mixtures. The TRI content was 0, 0.5%, 1.0%, and 1.5% by weight of cement, respectively. Therefore, there was a small difference between the values of CTE for TRI00, TRI05, TRI10, and TRI15 concretes. However, the total deformation in the cooling period consisted of both temperature deformation and autogenous deformation, and the presence of autogenous deformation would affect the accuracy of the CTE calculation results.

The AS was determined by Eq. (4) in this research, as recommended in [62].

$$\varepsilon_{as}(t) = \varepsilon_{tf}(t) - \alpha_T(t) \times [T(t) - T_{time-zero}] \tag{4}$$

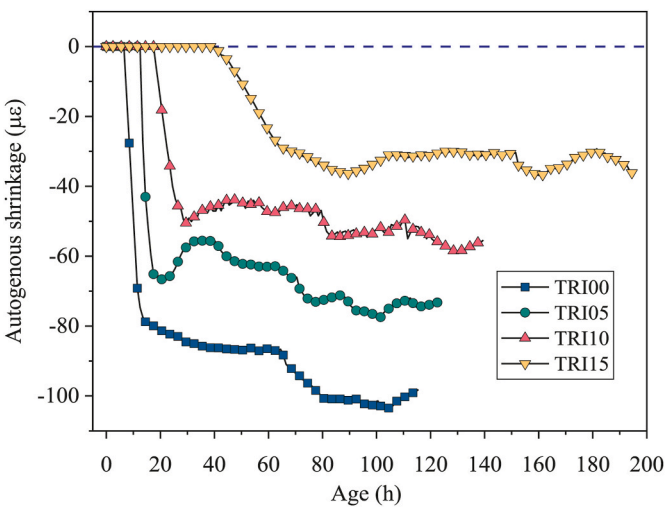

Fig. 9. AS of HSC with different TRI contents.

in which $\varepsilon_{as}(t)$ = time-dependent AS deformation, in με; and $T_{time-zero}$ = temperature of concrete at the starting point of AS, in °C.

Fig. 9 depicts the AS of HSC with different TRI contents. The AS zeroed to the moment when restrained stress occurred in four specimens. The development of AS of HSC with TRI included three stages, i.e., stages of rapid shrinkage, slow expansion, and slow shrinkage. However, the AS of reference concrete (TRI00) only had the stages of rapid shrinkage and slow shrinkage. Generally, the addition of TRI to HSC caused a decrease in AS when compared to that of reference concrete. Specifically, the absolute value of AS of TRI00 concrete at its cracking age (115.5 h) was 98 με, while HSC with 0.5%, 1.0%, and 1.5% TRI were 75, 52, and 32 με at the cracking age of TRI00 concrete, which decreased by 23.47%, 46.94%, and 67.35% with increasing TRI contents ranging from 0 to 0.5%, 1.0%, and 1.5%, respectively. The AS results are consistent with previous studies [13,63]. A possible explanation for this might be that the addition of TRI increases the dissolution rate of calcium, thus inhibiting the growth of ettringite crystals. The delayed growth of ettringite crystals leads to the decrease of AS strains [63].

By setting the temperature of the free shrinkage specimen to a constant of 20 °C for the TSTM test, the AS results can be obtained directly, which can be conducted in future studies to better investigate the AS of concrete and further verify the accuracy of Eq. (4). In this research, the main aim was to study the trend of the effect of TRI on the AS of concrete, so the current CTE calculation results are able to make a comparative analysis of the trend. In future studies, we need to specifically test the CTE of concrete in order to calculate the value of AS more accurately.

In this research, a modified prediction model for AS considering the effect of TRI contents on AS and time-zero of HSC was proposed, as given in Eq. (5) [64].

$$\begin{cases} \varepsilon_{cas}(t) = \varepsilon_{cas0}(\theta)\beta_a(t) \\ \beta_a(t) = 1 - \exp\left\{ -a \cdot [t - t_{cas0}(\theta)]^b \right\} \\ \varepsilon_{cas0}(\theta) = \varepsilon_{cas0}(0) \cdot f(\theta) \\ f(\theta) = \lambda_1\theta^2 + k_1\theta + c_1 \\ t_{cas0}(\theta) = t_{cas0}(0) \cdot \varphi(\theta) \\ \varphi(\theta) = \lambda_2\theta^2 + k_2\theta + c_2 \end{cases} \tag{5}$$

in which $\varepsilon_{cas}(t)$ = time-dependent AS, in με; $\varepsilon_{cas0}(\theta)$ = AS of HSC with different TRI contents at the cracking time of reference concrete (at 115.5 h), in με; $\beta_a(t)$ = development coefficient of AS; a, b = fitting parameters; θ = TRI content; $t_{cas0}(\theta)$ = time-zero of AS, in h; $\varepsilon_{cas0}(0)$ = AS of reference concrete at the cracking time; $f(\theta)$ = influence coefficient of AS; $t_{cas0}(0)$ = time-zero of AS of reference concrete, in h; $\varphi(\theta)$ = influence coefficient of time-zero; and λ, k, c = fitting parameters. The results of fitting parameters were obtained by nonlinear regression.

The average values of a and b were −0.3978, and 0.1277, respectively. The results of fitting parameters and coefficient of determination (R^2) of influence coefficients are depicted in Table 5.

The results of the prediction model for AS of HSC with TRI are depicted in Fig. 10. For instance, the results of AS at the cracking age of different specimens were −98, −73, −55, and −36 με for TRI00, TRI05, TRI10, and TRI15 concretes, respectively. The corresponding predicted results were −104, −79, −56, and −36 με, and the errors of the predicted and experimental results were 6.12%, 8.22%, 1.82%, and 0 for TRI00, TRI05, TRI10, and TRI15 concretes, respectively. Thus, the differences between the test results and the prediction model for AS were small, and the proposed model could express the effect of TRI contents on the development trends of AS clearly.

3.4. Early-age TC behavior of HSC with TRI

According to the superposition principle, the total strain is the sum of four terms: the autogenous strain, the elastic strain, and the basic creep strain, as given in Eq. (6) [53].

$$\varepsilon_{tr}(t) = \varepsilon_{as}(t) + \varepsilon_t(t) + \varepsilon_e(t) + \varepsilon_c(t) = \varepsilon_{sh}(t) + \varepsilon_e(t) + \varepsilon_c(t) \tag{6}$$

in which $\varepsilon_{tr}(t)$ = total deformation of restrained shrinkage specimen, which under a full restrained condition was to be zero, in με; $\varepsilon_{sh}(t)$ = free shrinkage strain consists AS, $\varepsilon_{as}(t)$, and thermal shrinkage, $\varepsilon_t(t)$, i.e., the total deformation of restrained shrinkage specimen, in με; $\varepsilon_c(t)$ = creep strain of restrained shrinkage specimen; and $\varepsilon_e(t)$ = elastic strain, which was the accumulation of tensile deformation during the process of shrinkage compensation of restrained shrinkage specimen, in με. The relationship between elastic strain, creep, and free shrinkage is depicted in Fig. 11. The creep of concrete consists of basic creep and drying creep. Only basic creep was considered in this research because all the concrete specimens were sealed immediately after pouring.

Basic TC was determined at the time when restrained tensile stress occurred. Specific TC is usually defined as the ratio of basic TC to unit stress (με/MPa) in a constant loading test [19]. Considering that the restrained stress developed over time in this research, thus the specific TC was defined as the ratio of cumulative basic TC to the corresponding restrained stress at an arbitrary time, as recommended in [40]. The specific TC of concrete could be determined utilizing Eq. (7) [6].

Table 5
Results of fitting parameters and coefficient of determination.

Fitting parameter	λ	k	c	R^2
$f(\theta)$	0.0306	−0.4969	1.0015	0.999
$\varphi(\theta)$	2.6154	−0.6308	1.1462	0.973

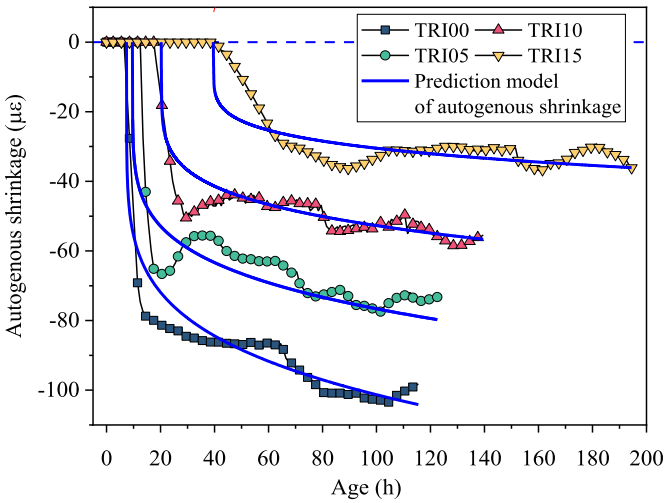

Fig. 10. Prediction model for AS of HSC with different TRI contents.

$$C_{sp}(t)=\frac{\Delta\varepsilon_c(t)}{\sigma_c(t)} \tag{7}$$

in which $C_{sp}(t)$ = specific TC at the age of t h, in με/MPa; $\Delta\varepsilon_c(t)$ = cumulative basic TC at the age of t h, in με; and $\sigma_c(t)$ = restrained stress at the age of t h, in MPa.

The stress develops when the shrinkage of concrete is under restrained condition, which would cause the concrete to creep in turn. Thus, the interaction of creep with shrinkage at early age is an important element in the deformation analysis of restrained concrete, which can be expressed as the ratio between the TC to free shrinkage, i.e., creep-shrinkage ratio [17]. The creep-shrinkage ratio is an element of great importance in evaluating the degree of stress relaxation because it reveals the reduction in the development of tensile strain in concrete under restrained condition [17,35,40]. The creep-shrinkage ratio was the ratio of basic TC to free shrinkage, as given in Eq. (8).

$$K(t)=\frac{\Delta\varepsilon_c(t)}{\varepsilon_{sh}(t)} \tag{8}$$

in which $K(t)$ = creep-shrinkage ratio at the age of t h; and $\varepsilon_{sh}(t)$ = free shrinkage strain at the age of t h, which was determined from the time when the restrained tensile stress occurred, in με.

Fig. 12 depicts that the compressive creep of TRI00, TRI05, and TRI10 concretes increased rapidly during the temperature rising period. TRI00, TRI05, and TRI10 concretes were subjected to compressive stress during the temperature rising period, which caused the development of compressive creep during this period. The TC of TRI15 concrete developed quickly after pouring. This result may be explained by the fact that the TRI15 concrete contracted and was pulled back to the origin position many times, as depicted in Fig. 8, and the elastic modulus of concrete was very low due to the hydration of cement being delayed. Thus, Although the restrained stress of TRI15 concrete was almost zero, the TRI concrete was under tensile condition for a long time, and the TC developed quickly.

The maximum absolute value of compressive creep of TRI00, TRI05, and TRI10 concretes was 150 (at 59.5h), 103 (at 63.5h), and

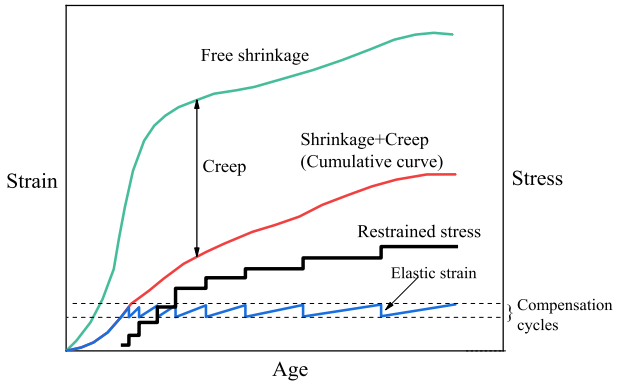

Fig. 11. Relationship between elastic strain, creep, and free shrinkage [65].

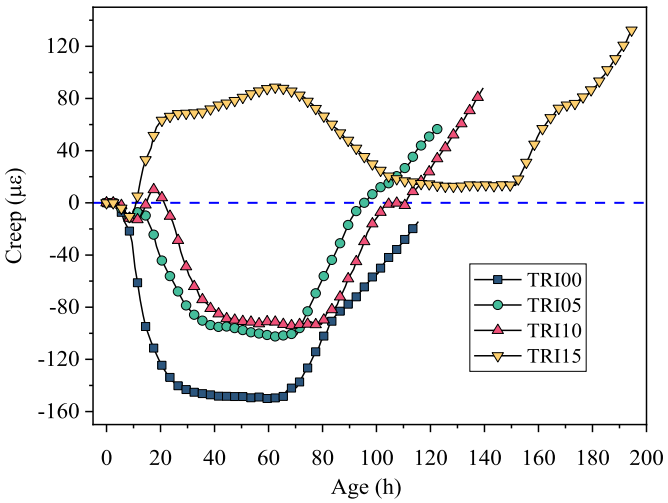

Fig. 12. Creep of HSC with different TRI contents.

94 με (at 70.5h), which decreased by 31.33%, and 37.33% with increasing TRI contents ranging from 0 to 0.5%, and 1.0%, respectively. TRI00, TRI05, and TRI10 concretes were subjected to compressive stress during the temperature rising period, which caused the development of compressive creep during this period. During the constant temperature curing period, the restrained compressive stress relaxed gradually, as depicted in Fig. 7. When the contents of TRI ranged from 0 to 0.5%, and 1.0%, the HSC specimens were subjected to compressive stress with a maximum value of 1.72 (at 23.5 h), 0.80 (at 31.5 h), and 0.61 MPa (at 44.5 h), respectively. The compressive stress at the starting points of cooling period were 0.86 (at 65.5h), 0.11 (at 70.5h), and 0.38 MPa (at 81.5h) for TRI00, TRI05, and TRI10 concretes, respectively. The rate of stress relaxation from the time of maximum compressive stress to the starting point of cooling period of TRI00, TRI05, and TRI10 concretes was 0.0204, 0.0177, 0.0062 MPa/h, which decreased by 13.24%, and 69.61% with increasing TRI contents ranging from 0 to 0.5%, and 1.0%, respectively. Then, the tensile stress developed quickly after the concrete entered the cooling period, which caused the TC to develop quickly during this period.

The results of basic TC of TRI00, TRI05, TRI10, and TRI15 concretes are depicted in Fig. 13. The TC development processes of four specimens were similar, and the basic TC strain at cracking age was 92, 89, 86, and 83 με, respectively. The basic TC developed from the time when the restrained stress in tension occurred. The basic TC, the average rate of basic TC, and the maximum absolute value of compressive creep all decreased with increasing TRI contents.

Fig. 14 depicts the development curves of basic TC of TRI00, TRI05, TRI10, and TRI15 concretes from the same starting point. The average rate of basic TC was 2.56, 2.28, 2.00, and 1.89 με/h for TRI00, TRI05, TRI10, and TRI15 concretes, which decreased by 10.94%, 21.88, and 26.17% with increasing TRI contents ranging from 0 to 0.5%, 1.0%, and 1.5%, respectively. Although the development period of basic TC was prolonged with increasing TRI contents, the basic TC at cracking age was still decreased by adding TRI due to the low development rate.

The specific TC calculated by Eq. (7) was used to eliminate the effect of various restrained stresses, and investigate the effect of TRI

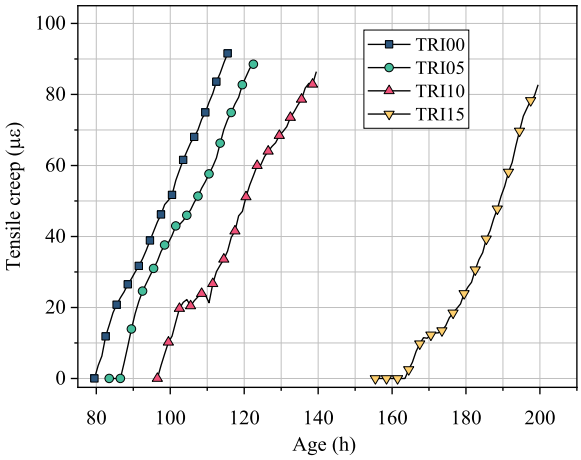

Fig. 13. Basic TC of HSC with different TRI contents.

content on early-age TC behavior, as depicted in Fig. 15. The specific TC of TRI00, TRI05, TRI10, and TRI15 concretes at cracking age was 48, 45, 41, and 37 με/MPa, which decreased by 6.25%, 14.58%, and 22.92% with increasing TRI contents ranging from 0 to 0.5%, 1.0%, and 1.5%, respectively. The results revealed that the addition of TRI decreased the TC of HSC in the long term.

The creep-shrinkage ratio of TRI00, TRI05, TRI10, and TRI15 concretes are depicted in Fig. 16. It could be found that the curves of creep-shrinkage ratio varied greatly at the early stage, and then decreased to be stable. Creep-shrinkage ratio decreased with increasing TRI contents ranging from 0 to 0.5%, and 1.0%, respectively. There was little difference between the stable values of TRI10 and TRI15 concretes. The result demonstrates that the degree of stress relaxation decreased by adding TRI, but there was little reduction in stress relaxation when the contents of TRI exceeded 1.0%.

The results of basic TC, specific TC, and creep-shrinkage ratio all decreased significantly by adding TRI, which revealed that the addition of TRI resisted the TC behavior of HSC. Generally, the stiffness of HSC at early age decreases by adding TRI, thus higher TC could be expected under direct tensile loading [3]. However, the development of TC in HSC with TRI was different from the traditional understanding that the TC increased with the addition of TRI due to the low stiffness when the HSC specimens were under restrained condition in this research. This result may be explained by the fact that the AS decreases by adding TRI, and the times that the restrained specimens are pulled back to original position decreases, thus inducing the decrease in the number of microcracks in the specimens [37]. The TC of concrete will decrease with the number of microcracks decrease under tensile condition [17]. Therefore, the TC of HSC under restrained condition decreased by adding TRI.

3.5. Evaluation of early-age cracking resistance of HSC with TRI

3.5.1. Cracking age, cracking temperature, and cracking stress

Quantitative criteria related to TSTM are taken to evaluate the cracking resistance of concrete under different test conditions [66]. In this research, single criteria and integrated criteria, i.e., cracking age, cracking temperature, cracking stress, and stress reserve were both taken to evaluate the early-age cracking resistance of HSC with TRI, as recommended in [27,37,66]. Table 6 depicts the results of single criteria of HSC with TRI. When the TRI content increased from 0 to 0.5%, 1.0%, and 1.5%, the cracking age or cracking stress of HSC increased by 6.06%, 20.78%, and 72.73% or 2.63%, 11.05%, and 16.32%, respectively. Cracking temperature of HSC decreased by 44.96%, 108.05%, and 109.24% with increasing TRI contents ranging from 0 to 0.5%, 1.0%, and 1.5%, respectively. The criterion of cracking temperature is proposed by RILEM that the higher cracking temperature indicates a higher potential for cracking at early age [67,68]. The results reveal that the early-age cracking resistance of HSC increased with increasing TRI contents.

3.5.2. Stress reserve

The stress reserve of concrete is taken to evaluate cracking resistance [27], which takes the stress at room temperature and cracking stress into consideration, as given in Eq. (9) [27,69]. Stress at room temperature is the response of concrete to temperature, deformation, and the degree of restraint. Cracking stress is the ultimate stress at which concrete resists cracking. Stress reserve reflects the ability of concrete to resist stress development after reaching room temperature, and if the ability to resist stress development is better, the cracking resistance is better [70].

$$\varphi = \frac{(\sigma_{cr} - \sigma_{rt})}{\sigma_{cr}} \times 100\% \tag{9}$$

in which φ = stress reserve;σ_{cr} = cracking stress, in MPa; and σ_{rt} = stress at room temperature, in MPa.

The stress at room temperature of TRI00, TRI05, TRI10, and TRI15 concretes was 1.76, 1.34, 0.98, and 0.80 MPa, respectively, which can be obtained in Figs. 5 and 7. The results of stress reserve of HSC with different TRI contents at early age are depicted in Fig. 17. The stress reserve was calculated by Eq. (9), and the results were 0.074, 0.313, 0.536, and 0.638 for TRI00, TRI05, TRI10, and

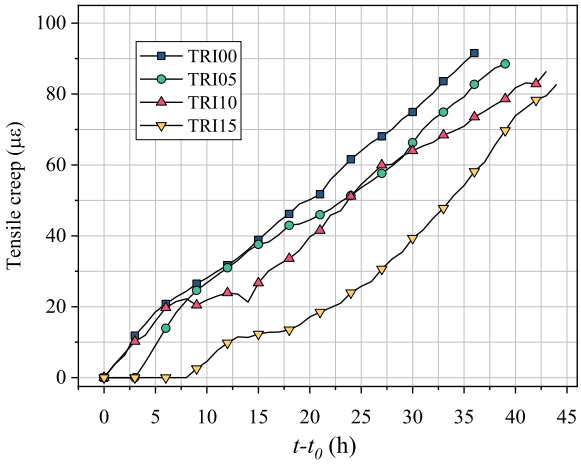

Fig. 14. Development curves of basic TC.

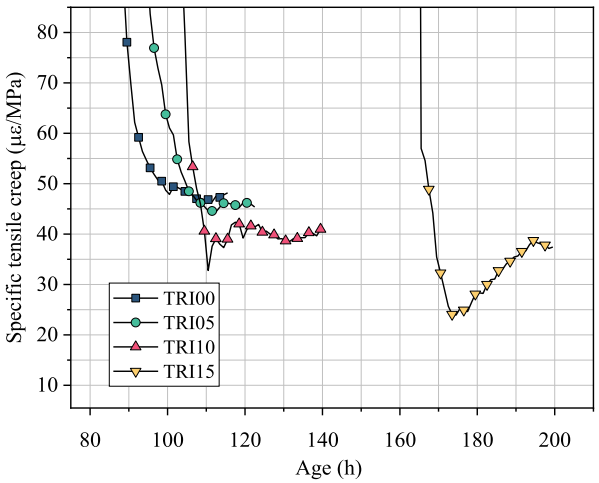

Fig. 15. Specific TC of HSC with different TRI contents.

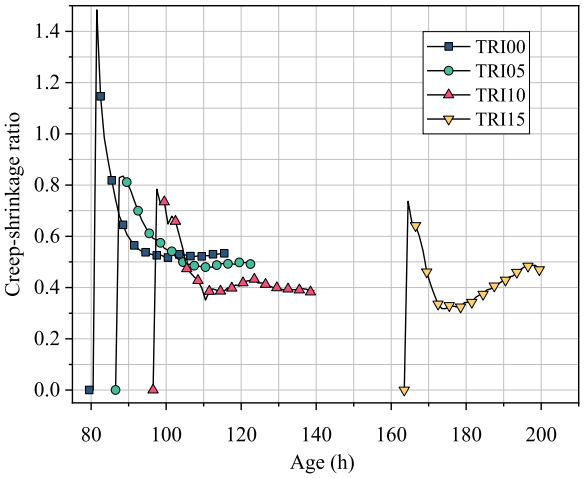

Fig. 16. Creep-shrinkage ratio of HSC with different TRI contents.

Table 6
Cracking age and cracking stress of HSC with TRI.

Item	Unit	TRI00	TRI05	TRI10	TRI15
Cracking age	h	115.5	122.5	139.5	199.5
Cracking temperature	°C	16.77	9.23	−1.35	−1.55
Cracking stress	MPa	1.90	1.95	2.11	2.21

TRI15 concretes, which increased by 322.97%, 624.32%, and 762.16% with increasing TRI contents ranging from 0 to 0.5%, 1.0%, and 1.5%, respectively.

The results revealed that a higher stress reserve indicates higher cracking resistance [27]. Although the addition of TRI improved the stress reserve, the degree of improvement of TRI for the stress reserve decreased with the increase of the total TRI contents. When the total TRI contents were 0, 0.5%, and 1.0%, the increments of stress reserve were 0.239, 0.223, and 0.102 by adding 0.5% TRI content, as depicted in Fig. 17. In summary, the addition of TRI improved the early-age cracking resistance of HSC, and the degree of improvement of TRI for the cracking resistance decreased with increasing total TRI contents.

3.6. The modified stress-strain failure criterion

Failure criteria include stress-based, strain-based, and stress-strain combined criteria. However, the cracking strain of HSC reaches its strain capacity when cracks appear, and the cracking stress was lower than its strength capacity. The stress-based and strain-based criteria have different rules for judging the thermal cracking resistance of concrete [71]. Thus, to estimate the safety of single

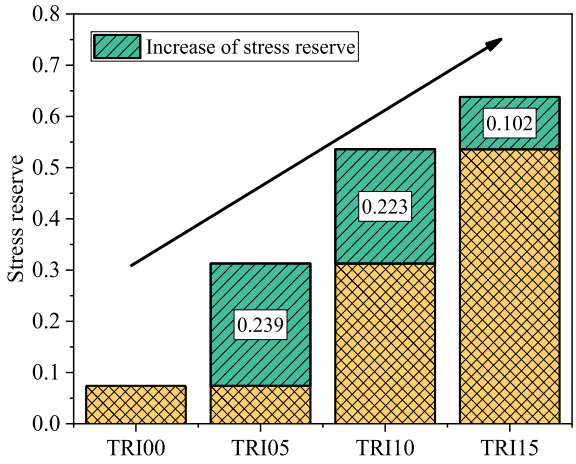

Fig. 17. Stress reserve of HSC with different TRI contents.

restrained concrete considering strain and stress simultaneously, a stress-strain failure criterion was proposed in this research. Zhu et al. [72] proposed a universal stress-strain failure criterion, which assumed that the failure energies of different loading paths were the same at cracking time. The criterion proposed by Zhu et al. was based on data measured in the direct tensile test and restrained cracking test. In this research, the theoretical failure results calculated from prediction models for mechanical properties of HSC were used to replace the results of the direct tensile test, and the results of the restrained cracking test were obtained by TSTM. The strain energy of the restrained cracking and theoretical direct tension cracking can be calculated by Eq. (10) under the assumption of equal failure energy [72]. Eq. (11) depicts the modified stress-strain failure criterion in this research, and Fig. 18 depicts the stress-strain relationship between the results of the restrained cracking test and theoretical failure results.

$$W_0 + W_1 = \int_0^{\varepsilon_p} \sigma_p(\varepsilon)\, d\varepsilon = \int_0^{\varepsilon_{cr}} \sigma_{cr}(\varepsilon)\, d\varepsilon = W_0 + W_2 \tag{10}$$

$$f(\varepsilon_c, \sigma_c) = k \cdot E_p \cdot (\varepsilon_c - \varepsilon_p) - (\sigma_p - \sigma_c) \tag{11}$$

in which $f(\varepsilon_c,\sigma_c)$ = the modified stress-strain failure criterion; k = relationship between σ_c and σ_p under the linear assumption; E_p = theoretical result of elastic modulus at equivalent cracking age, in Gpa; ε_c = accumulative strain of restrained concrete at the cracking age, in με; σ_p = theoretical result of stress at equivalent cracking age, in MPa; and ε_p = theoretical result of strain at equivalent cracking age, in με. Concrete is safe when the value of $f(\varepsilon_c,\sigma_c)$ is less than 0, and concrete is likely to crack when the value of $f(\varepsilon_c,\sigma_c)$ is over 0.

The stress and strain of restrained concrete at the cracking age were determined by the TSTM. The axial tensile strength could be calculated by Eq. (12) based on the results of splitting tensile strength, as recommended in [73,74]. The theoretical results of stress σ_p and strain ε_p at equivalent cracking age were obtained by using Eq. (13).

$$f_t = 0.77 \times f_{spl} + 0.21 \tag{12}$$

$$\begin{cases} \sigma_p = \eta \cdot f_{t,c} \\ \varepsilon_p = \dfrac{\sigma_p}{E_{t,c}} \end{cases} \tag{13}$$

in which f_t = axial tensile strength, in MPa; f_{spl} = splitting tensile strength, in MPa; η = relationship between cracking stress and tensile strength; $f_{t,c}$ = axial tensile strength at the equivalent cracking age of concrete cured under 20 °C, in MPa; $E_{t,c}$ = elastic modulus of concrete under direct tensile loading at the equivalent cracking age cured under 20 °C, in GPa; and η was the ratio of elastic modulus of concrete under restrained condition and elastic modulus under direct tensile loading at the equivalent cracking age cured under 20 °C in this research.

The equivalent age of concrete cured under 20 °C can be calculated by Eq. (14) [75,76].

$$t_e = \int_0^t \exp\left[\frac{E_a(T)}{R}\left(\frac{1}{T_{ref}+273} - \frac{1}{T(t)+273}\right)\right] dt \tag{14}$$

in which t = age of concrete after pouring, in d; $E_a(T)$ = activation energy, in kJ/molkJ/mol ($T(t) \geq 20\ ^\circ C$, $E_a(T) = 33.5$ kJ/ mol; $T(t) < 20\ ^\circ C$, $E_a(T) = 33.5 + 1.47(20 - T(t))$ kJ/mol); R = an ideal gas constant (8.315 $J \cdot mol^{-1} \cdot K^{-1}$); T_{ref} = reference temperature (20 °C); and $T(t)$ = time-dependent temperature, in °C. The addition of TRI would affect the value of activation energy. In this research, the calculation is simplified by assuming the activation energy to be a constant when the temperature was over 20 °C. It is important to

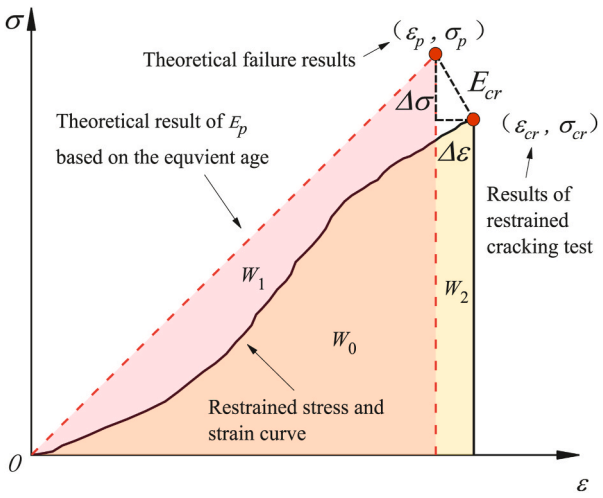

Fig. 18. Stress-strain relationships of theoretical failure results and results of restrained cracking test.

conduct experiments to measure the activation energy of concrete containing different TRI contents in further studies in order to improve the accuracy of calculating equivalent age.

In this research, the predicted results of axial tensile strength or elastic modulus at equivalent cracking age were based on the prediction models of axial tensile strength and elastic modulus proposed in [73,74,77], as given in Eqs. (15) and (16).

$$f_t(t) = f_{t,28} \exp\left[S_1\left(1-\sqrt{\frac{28}{t}}\right)\right] \tag{15}$$

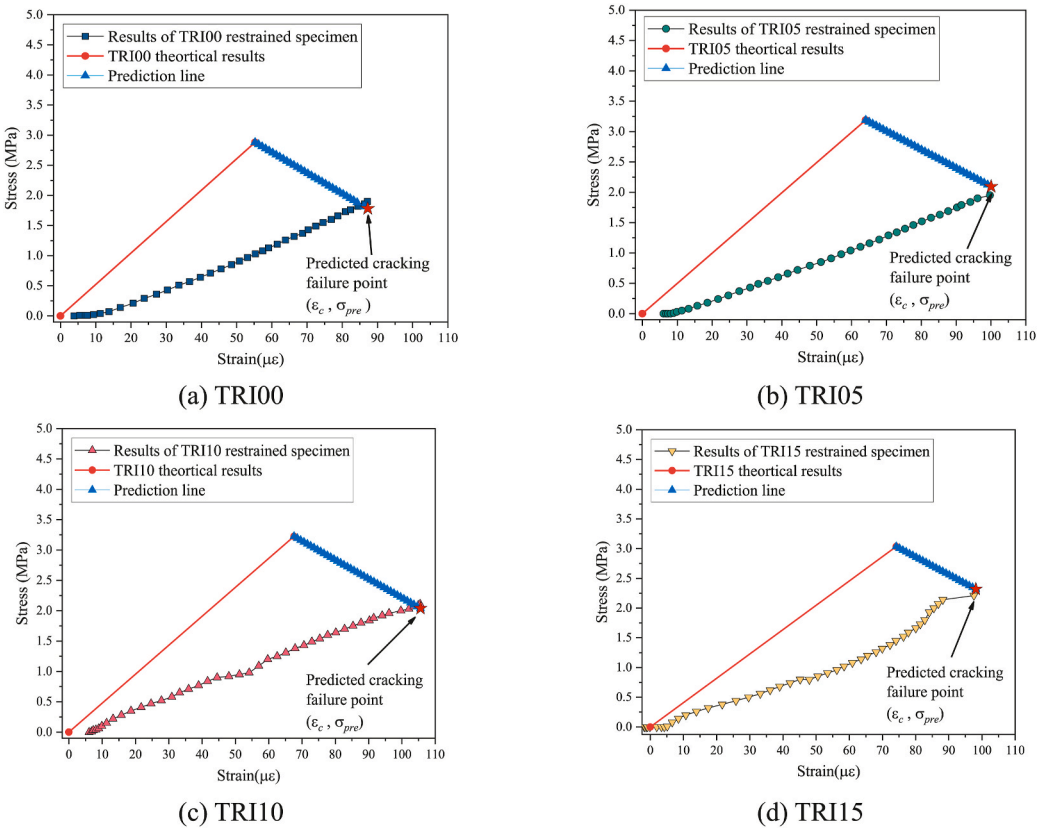

Fig. 19. Stress-strain relationships of four specimens.

$$E_c(t) = E_{c,28} \exp\left[S_2\left(1 - \sqrt{\frac{28}{t}}\right)\right] \tag{16}$$

in which $f_{t,28}$ = 28-d axial tensile strength, in MPa; $E_{c,28}$ = 28-d elastic modulus, in GPa; and S_1, S_2 = fitting parameters. The results of fitting parameter S_1 were 0.063, 0.067, 0.096, and 0.283 for TRI00, TRI05, TRI10, and TRI15 concretes, respectively. The predicted results of axial tensile strength at equivalent cracking age, $f_{t,c}$, were obtained by inputting the results of equivalent cracking age of TRI00, TRI05, TRI10, and TRI15 concretes. The results of fitting parameter S_2 were 0.133, 0.147, 0.156, and 0.262 for TRI00, TRI05, TRI10, and TRI15 concretes, respectively. The predicted results of elastic modulus at equivalent cracking age, $E_{t,c}$, were obtained by inputting the results of equivalent cracking age of TRI00, TRI05, TRI10, and TRI15 concretes.

The predicted results of axial tensile strength or elastic modulus at equivalent cracking age were 3.21, 3.10, 3.09, and 2.80 MPa or 52.17, 49.81, 47.69, 40.92 GPa for TRI00, TRI05, TRI10, and TRI15 concretes, respectively. The theoretical results of stress σ_p and strain ε_p at equivalent cracking age could be obtained after determining the predicted results of axial tensile strength and elastic modulus at equivalent cracking age.

The prediction accuracy of the modified stress-strain failure criterion proposed in this research was evaluated by comparing the predicted results of cracking stress to that obtained by TSTM test. By substituting k and ε_c into Eq. (11), the predicted failure stress σ_{pre} was derived. The predicted cracking failure point (ε_c,σ_{pre}) has been highlighted in Fig. 19 with red pentagram. The prediction line in Fig. 19 is obtained by Eq. (11).

Table 7 depicts the theoretical failure results and results of the restrained cracking test of TRI00, TRI05, TRI10, and TRI15 concretes, respectively. The predicted cracking stress could be calculated by substituting the results of k, σ_p, ε_p, and ε_{cr} in Eq. (11). The relative prediction error between σ_{pre} and σ_c ranged from −6.32% to 4.98%, which was acceptable in practical engineering. On the whole, the modified stress-strain failure criterion could be used to predict the cracking stress of HSC with TRI. The modified stress-strain failure criterion could obtain the results from the restrained cracking tests and prediction models for mechanical properties, and the direct tensile test is not needed in this research. In practical engineering, the modified stress-strain failure criterion has certain significance to design a better temperature control strategy for increasing the cracking resistance of concrete.

4. Conclusion

The aim of this research was to investigate the effect of TRI contents on the early-age behavior and cracking resistance of HSC under uniaxial restrained condition and propose a criterion for evaluating the cracking resistance of a single concrete mixture.

The efficacy of TRI on the reduction of temperature rise, AS, and TC was measured in concrete elements. The addition of TRI reduced the peak temperature of concrete obviously, and the temperature rising rate decreased by adding TRI. The TC, creep-shrinkage ratio, and specific TC of HSC were reduced by adding TRI. The mechanical properties of HSC decreased with increasing TRI contents, and the gap between HSC with different TRI contents was small at 28 d. The addition of TRI reduced the AS at early age, and a prediction model for AS considering the effect of TRI contents on AS and time-zero of HSC was proposed.

The efficacy of TRI contents in improving the early-age cracking resistance of HSC was quantitatively evaluated. A stress-strain failure criterion for concrete under the assumption of equal failure energy was proposed. The relative prediction error ranged from −6.32% to 4.98% in this research. Future studies will be conducted using the criterion to better evaluate the cracking resistance of concrete in practical engineering.

CRediT author statement

Dejian Shen: Conceptualization, Methodology, Project administration. Jiacheng Kang: Investigation, Writing – original draft, Writing-Reviewing and Editing, Formal analysis. Ci Liu: Investigation, Validation. Ming Li: Validation. Yifan Wei: Writing – original draft, Validation. Liukun Zhou: Investigation, Validation.

Declaration of competing interest

The authors declare that they have no known competing financial interests or personal relationships that could have appeared to influence the work reported in this paper

Table 7
Experimental and predicted results.

Concrete mixtures	Restrained specimen		Theoretical results		$k = \frac{\sigma_c}{\sigma_p}$	σ_{pre}	$\frac{\sigma_{pre} - \sigma_c}{\sigma_c}$
	σ_c	ε_c	σ_p	ε_p			
TRI00	1.90	89	2.88	55	0.66	1.78	−6.32%
TRI05	1.95	100	3.16	63	0.62	2.02	3.59%
TRI10	2.11	105	3.22	68	0.66	2.04	−3.32%
TRI15	2.21	98	3.03	74	0.73	2.32	4.98%

Data availability

Data will be made available on request.

Acknowledgements

The financial support of the National Natural Science Foundation of China (Grant No. 51879092) is gratefully acknowledged. The Postgraduate Research & Practice Innovation Program of Jiangsu Province (Grant No. KYCX22_0614) is also gratefully acknowledged. The support of the Fundamental Research Funds for the Central Universities (Grant No 2019B52814) is gratefully acknowledged. This work is also supported by Science and Technology Planning Project of Jiangsu Province (Grant No. BE2022605).

References

[1] H. Zhang, L. Li, P. Feng, W.B. Wang, Q. Tian, J.P. Liu, Impact of Temperature Rising Inhibitor on hydration kinetics of cement paste and its mechanism, Cem. Concr. Compos. 93 (2018) 289–300, https://doi.org/10.1016/j.cemconcomp.2018.07.018.
[2] Y. Yan, A. Ouzia, C. Yu, J.P. Liu, K.L. Scrivener, Effect of a novel starch-based temperature rise inhibitor on cement hydration and microstructure development, Cement Concr. Res. 129 (2020), 105961, https://doi.org/10.1016/j.cemconres.2019.105961.
[3] M. Li, W. Xu, Y.J. Wang, Q. Tian, J.P. Liu, Shrinkage crack inhibiting of cast in situ tunnel concrete by double regulation on temperature and deformation of concrete at early age, Construct. Build. Mater. 240 (2020), 117834, https://doi.org/10.1016/j.conbuildmat.2019.117834.
[4] N. Banthia, N. Nandakumar, Crack growth resistance of hybrid fiber reinforced cement composites, Cem. Concr. Compos. 25 (1) (2003) 3–9, https://doi.org/10.1016/S0958-9465(01)00043-9.
[5] D.J. Shen, C. Liu, C.Y. Wen, J.C. Kang, M. Li, H. Jiang, Restrained cracking failure behavior of concrete containing MgO compound expansive agent under adiabatic condition at early age, Cem. Concr. Compos. 135 (2023) 104825, https://doi.org/10.1016/j.cemconcomp.2022.104825.
[6] D. Cusson, T. Hoogeveen, An experimental approach for the analysis of early-age behaviour of high-performance concrete structures under restrained shrinkage, Cement Concr. Res. 37 (2) (2007) 200–209, https://doi.org/10.1016/j.cemconres.2006.11.005.
[7] J. Kheir, A. Klausen, T.A. Hammer, L. De Meyst, B. Hilloulin, K. Van Tittelboom, A. Loukili, N. De Belie, Early age autogenous shrinkage cracking risk of an ultra-high performance concrete (UHPC) wall: modelling and experimental results, Eng. Fract. Mech. 257 (2021), 108024, https://doi.org/10.1016/j.engfracmech.2021.108024.
[8] L. Wang, G.X. Li, X. Li, F.X. Guo, S.W. Tang, X. Lu, A. Hanif, Influence of reactivity and dosage of MgO expansive agent on shrinkage and crack resistance of face slab concrete, Cem. Concr. Compos. 126 (2022), 104333, https://doi.org/10.1016/j.cemconcomp.2021.104333.
[9] L.M. Wu, N. Farzadnia, C.J. Shi, Z.H. Zhang, H. Wang, Autogenous shrinkage of high performance concrete: a review, Construct. Build. Mater. 149 (2017) 62–75, https://doi.org/10.1016/j.conbuildmat.2017.05.064.
[10] Y. Yan, R. Wang, J.P. Liu, J.H. Tang, K.L. Scrivener, Effect of a liquid-type temperature rise inhibitor on cement hydration, Cement Concr. Res. 140 (2021), 106286, https://doi.org/10.1016/j.cemconres.2020.106286.
[11] H. Zhang, W.B. Wang, Q.L. Li, Q. Tian, L. Li, Jp Liu, A starch-based admixture for reduction of hydration heat in cement composites, Construct. Build. Mater. 173 (2018) 317–322, https://doi.org/10.1016/j.conbuildmat.2018.03.199.
[12] H. Zhang, X. Liu, P. Feng, L. Li, W.B. Wang, Influence of temperature rising inhibitor on nucleation and growth process during cement hydration, Thermochim. Acta 681 (2019), 178403, https://doi.org/10.1016/j.tca.2019.178403.
[13] H. Zhang, W. She, L. Li, W.B. Wang, Effect of temperature rising inhibitor on autogenous shrinkage of cement pastes, Construct. Build. Mater. 220 (2019) 329–339, https://doi.org/10.1016/j.conbuildmat.2019.06.044.
[14] X.Z. Wang, M.S. Shi, X.G. Wang, Application of hydration heat inhibitor in crack control of mass concrete of tunnel side wall, E3S Web of Conferences 283 (2021), 01032, https://doi.org/10.1051/e3sconf/202128301032.
[15] D.J. Shen, J.L. Jiang, W.T. Wang, J.X. Shen, G.Q. Jiang, Tensile creep and cracking resistance of concrete with different water-to-cement ratios at early age, Construct. Build. Mater. 146 (2017) 410–418, https://doi.org/10.1016/j.conbuildmat.2017.04.056.
[16] I. Khan, A. Castel, R.I. Gilbert, Tensile creep and early-age concrete cracking due to restrained shrinkage, Construct. Build. Mater. 149 (2017) 705–715, https://doi.org/10.1016/j.conbuildmat.2017.05.081.
[17] S.A. Altoubat, D.A. Lange, Creep, shrinkage, and cracking of restrained concrete at early age, ACI Mater. J. 98 (4) (2001) 323–331.
[18] B. Bissonnette, M. Pigeon, Tensile creep at early ages of ordinary, silica fume and fiber reinforced concretes, Cement Concr. Res. 25 (5) (1995) 1075–1085, https://doi.org/10.1016/0008-8846(95)00102-I.
[19] K. Kolver, S. Igarashi, A. Bentur, Tensile creep behavior of high strength concretes at early ages, Mater. Struct. 32 (5) (1999) 383–387, https://doi.org/10.1007/BF02479631.
[20] D.H. Nguyen, V.T. Nguyen, P. Lura, V.T. Dao, Temperature-stress testing machine-A state-of-the-art design and its unique applications in concrete research, Cem. Concr. Compos. 102 (2019) 28–38, https://doi.org/10.1016/j.cemconcomp.2019.04.019.
[21] L. Li, V. Dao, P. Lura, Autogenous deformation and coefficient of thermal expansion of early-age concrete: initial outcomes of a study using a newly-developed Temperature Stress Testing Machine, Cem. Concr. Compos. 119 (2021), 103997, https://doi.org/10.1016/j.cemconcomp.2021.103997.
[22] T.J. Barrett, I. De la Varga, W.J. Weiss, Reducing cracking in concrete structures by using internal curing with high volumes of fly ash, Struct. Congr. 2012 (2012) 699–707, https://doi.org/10.1061/9780784412367.063.
[23] K.A. Riding, J.L. Poole, A.K. Schindler, M.C. Juenger, K.J. Folliard, Quantification of effects of fly ash type on concrete early-age cracking, ACI Mater. J. 105 (2) (2008) 149–155.
[24] A. Markandeya, N. Shanahan, D.M. Gunatilake, K.A. Riding, A. Zayed, Influence of slag composition on cracking potential of slag-portland cement concrete, Construct. Build. Mater. 164 (2018) 820–829, https://doi.org/10.1016/j.conbuildmat.2017.12.216.
[25] S. Tongaroonsri, S. Tangtermsirikul, Effect of mineral admixtures and curing periods on shrinkage and cracking age under restrained condition, Construct. Build. Mater. 23 (2) (2009) 1050–1056, https://doi.org/10.1016/j.conbuildmat.2008.05.023.
[26] T. Meagher, N. Shanahan, D. Buidens, K.A. Riding, A. Zayed, Effects of chloride and chloride-free accelerators combined with typical admixtures on the early-age cracking risk of concrete repair slabs, Construct. Build. Mater. 94 (2015) 270–279, https://doi.org/10.1016/j.conbuildmat.2015.07.003.
[27] N.N. Shi, J.S. Ouyang, R.X. Zhang, D.H. Huang, Experimental study on early-age crack of mass concrete under the controlled temperature history, Adv. Mater. Sci. Eng. 12 (3) (2014) 352–358, https://doi.org/10.1155/2014/671795.
[28] GB/T 14685-2011, Pebble and Crushed Stone for Construction, Ministry of Housing and Urban-Rural Development of the People Republic of China, 2011 (in Chinese).
[29] ASTM C150/C150M-20, Standard Specification for Portland Cement, ASTM International, West Conshohocken, PA, 2020.
[30] ASTM C191-21, Standard T Est Methods for Time of Setting of Hydraulic Cement by Vicat Needle, ASTM International, West Conshohocken, PA, USA, 2021.
[31] ASTM C143/C143M-12, Standard T Est Method for Slump of Hydraulic-Cement Concrete, ASTM International, West Conshohocken, PA, USA, 2015.
[32] GB/T 50081-2019, Standard for Test Methods of Concrete Physical and Mechanical Properties, Ministry of Housing and Urban-Rural Development of the People Republic of China, 2019 (in Chinese).
[33] J.D. Xin, Y. Liu, G.X. Zhang, Z.H. Wang, J. Wang, N. Yang, Y. Qiao, Evaluation of early-age thermal cracking resistance of high w/b, high volume fly ash (HVFA) concrete using temperature stress testing machine, Case Stud. Constr. Mater. 16 (2022), e00825, https://doi.org/10.1016/j.cscm.2021.e00825.

[34] L.L. Liu, J.S. Ou Yang, F.L. Li, J.D. Xin, D.H. Huang, S.L. Gao, Research on the Crack Risk of Early-Age Concrete under the Temperature Stress Test Machine, Mater., 2018.
[35] T. Zhang, W.Z. Qin, Tensile creep due to restraining stresses in high-strength concrete at early ages, Cement Concr. Res. 36 (3) (2006) 584–591, https://doi.org/10.1016/j.cemconres.2005.11.017.
[36] D.J. Shen, W.T. Wang, Q.Y. Li, P.P. Yao, G.Q. Jiang, Early-age behaviour and cracking potential of fly ash concrete under restrained condition, Mag. Concr. Res. 72 (5) (2020) 246–261, https://doi.org/10.1680/jmacr.18.00106.
[37] D.J. Shen, J.C. Kang, Y. Jiao, M. Li, C.C. Li, Effects of different silica fume dosages on early-age behavior and cracking resistance of high strength concrete under restrained condition, Construct. Build. Mater. 263 (2020), 120218, https://doi.org/10.1016/j.conbuildmat.2020.120218.
[38] Y. Wei, W. Hansen, Tensile creep behavior of concrete subject to constant restraint at very early ages, J. Mater. Civ. Eng. 25 (9) (2013) 1277–1284, https://doi.org/10.1061/(asce)mt.1943-5533.0000671.
[39] I. Pane, W. Hansen, Predictions and verifications of early-age stress development in hydrating blended cement concrete, Cement Concr. Res. 38 (11) (2008) 1315–1324, https://doi.org/10.1016/j.cemconres.2008.05.001.
[40] Z.F. Zhao, K.J. Wang, D.A. Lange, H.G. Zhou, W.L. Wang, D.M. Zhu, Creep and thermal cracking of ultra-high volume fly ash mass concrete at early age, Cem. Concr. Compos. 99 (2019) 191–202, https://doi.org/10.1016/j.cemconcomp.2019.02.018.
[41] J.D. Xin, S.Q. Lin, N.N. Shi, J.S. Ou Yang, D.H. Huang, Effect of reinforcement on early-age concrete temperature stress: preliminary experimental investigation and analytical simulation, Adv. Mater. Sci. Eng. 2015 (2015) 1–9, https://doi.org/10.1155/2015/231973.
[42] J.D. Xin, G.X. Zhang, Y. Liu, Z.H. Wang, Z. Wu, Effect of temperature history and restraint degree on cracking behavior of early-age concrete, Construct. Build. Mater. 192 (2018) 381–390, https://doi.org/10.1016/j.conbuildmat.2018.10.066.
[43] A. Bentur, Early-age shrinkage and cracking in cementitious systems, Concr. Sci. Eng. 3 (2001) 3–12.
[44] P. Lura, K. Van Breugel, I. Maruyama, Effect of curing temperature and type of cement on early-age shrinkage of high-performance concrete, Cement Concr. Res. 31 (12) (2001) 1867–1872, https://doi.org/10.1016/S0008-8846(01)00601-9.
[45] A. Darquennes, S. Staquet, B. Espion, Determination of time-zero and its effect on autogenous deformation evolution, Eur. J. Environ. Civ. En. 15 (7) (2011) 1017–1029, https://doi.org/10.1080/19648189.2011.9695290.
[46] H. Huang, G. Ye, Examining the "time-zero" of autogenous shrinkage in high/ultra-high performance cement pastes, Cement Concr. Res. 97 (2017) 107–114, https://doi.org/10.1016/j.cemconres.2017.03.010.
[47] Y. Ma, X. Yang, J. Hu, Z. Zhang, H. Wang, Accurate determination of the "time-zero" of autogenous shrinkage in alkali-activated fly ash/slag system, Compos. B Eng. 177 (2019), 107367, https://doi.org/10.1016/j.compositesb.2019.107367.
[48] J.R. Tenório Filho, M.A. Pereira Gomes de Araújo, D. Snoeck, N. De Belie, Discussing different approaches for the time-zero as start for autogenous shrinkage in cement pastes containing superabsorbent polymers, Materials 12 (18) (2019) 2962–2977, https://doi.org/10.3390/ma12182962.
[49] M.S. Meddah, A. Tagnit-Hamou, Evaluation of rate of deformation for early-age concrete shrinkage analysis and time zero determination, J. Mater. Civ. Eng. 23 (7) (2011) 1076–1086, https://doi.org/10.1061/(ASCE)MT.1943-5533.0000261.
[50] C.W. Miao, Q. Tian, J.P. Liu, W. Sun, Very early age self-desiccation effect measurement based on meniscus depression technology for concrete, J. Chin. Ceram. Soc. 35 (4) (2007) 509–516 (in Chinese).
[51] S. Eppers, C. Mueller, Autogenous shrinkage and time-zero of UHPC determined with the shrinkage cone, Proceed. Concreep 8 (2008) 709–714.
[52] M.S. Meddah, P.C. Aïtcin, N. Petrov, A new approach for the determination of the starting point of autogenous shrinkage strains (ASS), Spec. Publ. 234 (2006) 473–484.
[53] B. Delsaute, New Approach for Monitoring and Modeling of the Creep and Shrinkage Behaviour of Cement Pastes, Mortars and Concretes since Setting Time, 2016. Paris Est.
[54] A.E. Klausen, T. Kanstad, O. Bjøntegaard, E.J. Sellevold, The effect of curing temperature on autogenous deformation of fly ash concretes, Cem. Concr. Compos. 109 (2020), https://doi.org/10.1016/j.cemconcomp.2020.103574.
[55] E.J. Sellevold, O. Bjøntegaard, Coefficient of thermal expansion of cement paste and concrete: mechanisms of moisture interaction, Mater. Struct. 39 (9) (2006) 809–815, https://doi.org/10.1617/s11527-006-9086-z.
[56] D.J. Shen, J.L. Jiang, Y. Jiao, J.X. Shen, G.Q. Jiang, Early-age tensile creep and cracking potential of concrete internally cured with pre-wetted lightweight aggregate, Construct. Build. Mater. 135 (2017) 420–429, https://doi.org/10.1016/j.conbuildmat.2016.12.187.
[57] H.T. Zhao, Y. Xiang, X.D. Chen, J. Huang, W. Xu, H. Li, Y.J. Wang, P.G. Wang, Mechanical properties and volumetric deformation of early-age concrete containing CaO-MgO blended expansive agent and temperature rising inhibitor, Construct. Build. Mater. 299 (2021), 123977, https://doi.org/10.1016/j.conbuildmat.2021.123977.
[58] J. Zhang, H.D. Wei, S. Wei, Experimental study on the relationship between shrinkage and interior humidity of concrete at early age, Mag. Concr. Res. 62 (3) (2010) 191–199, https://doi.org/10.1680/macr.2010.62.3.191.
[59] M. Viviani, B. Glisic, I. Smith, Separation of thermal and autogenous deformation at varying temperatures using optical fiber sensors, Cem. Concr. Compos. 29 (6) (2007) 435–447, https://doi.org/10.1016/j.cemconcomp.2007.01.005.
[60] Z.F. Zhao, J.P. Chen, W.L. Wang, Determination of thermal expansion coefficient of concrete dosed with different volumes of fly ash, J. Yangtze River Sci. Res. Inst. 35 (12) (2018) 143–147 (in Chinese), http://ckyyb.crsri.cn/CN/10.11988/ckyyb.20180019.
[61] B. Delsaute, S. Staquet, Decoupling thermal and autogenous strain of concretes with different water/cement ratios during the hardening process, Adv. civil eng. mater. 6 (2) (2017) 1–22, https://doi.org/10.1520/ACEM20160063.
[62] I. Chu, S.H. Kwon, M.N. Amin, J.-K. Kim, Estimation of temperature effects on autogenous shrinkage of concrete by a new prediction model, Construct. Build. Mater. 35 (2012) 171–182, https://doi.org/10.1016/j.conbuildmat.2012.03.005.
[63] H. Zhang, L. Li, W.B. Wang, Effects of temperature rising inhibitor on nucleation and growth process of ettringite, J. Solid State Chem. 274 (2019) 222–228, https://doi.org/10.1016/j.jssc.2019.03.037.
[64] E. Tazawa, S. Miyazawa, Influence of cement and admixture on autogenous shrinkage of cement paste, Cement Concr. Res. 25 (2) (1995) 281–287, https://doi.org/10.1016/0008-8846(95)00010-0.
[65] K. Kovler, Testing system for determining the mechanical behaviour of early age concrete under restrained and free uniaxial shrinkage, Mater. Struct. 27 (6) (1994) 324–330, https://doi.org/10.1007/BF02473424.
[66] J.D. Xin, G.X. Zhang, Y. Liu, Z.H. Wang, Z. Wu, Evaluation of behavior and cracking potential of early-age cementitious systems using uniaxial restraint tests: a review, Construct. Build. Mater. 231 (2020), 117146, https://doi.org/10.1016/j.conbuildmat.2019.117146.
[67] Springenschmid R, Prevention of Thermal Cracking in Concrete at Early Ages, CRC Press2004.
[68] R. Breitenbücher, Investigation of thermal cracking with the cracking-frame, Mater. Struct. 23 (3) (1990) 172–177, https://doi.org/10.1007/BF02473015.
[69] D.J. Shen, J.L. Jiang, J.X. Shen, P.P. Yao, G.Q. Jiang, Influence of curing temperature on autogenous shrinkage and cracking resistance of high-performance concrete at an early age, Construct. Build. Mater. 103 (2016) 67–76, https://doi.org/10.1016/j.conbuildmat.2015.11.039.
[70] G.Z. Zhang, L.Q. Tu, W.H. Xia, K.X. Liu, B.J. Liu, Study on evaluation index of early ages cracking in concrete, Concr 5 (37) (2005) 13–17 (in Chineses).
[71] H. Zhu, Y. Hu, R. Ma, J. Wang, Q.B. Li, Concrete thermal failure criteria, test method, and mechanism: a review, Construct. Build. Mater. 283 (2021), 122762, https://doi.org/10.1016/j.conbuildmat.2021.122762.
[72] H. Zhu, Y. Hu, Q.B. Li, R. Ma, Restrained cracking failure behavior of concrete due to temperature and shrinkage, Construct. Build. Mater. 244 (2020), https://doi.org/10.1016/j.conbuildmat.2020.118318.
[73] T. Kanstad, T.A. Hammer, O. Bjøntegaard, E.J. Sellevold, Mechanical properties of young concrete: Part II: determination of model parameters and test program proposals, Mater. Struct. 36 (4) (2003) 226–230, https://doi.org/10.1007/BF02479615.
[74] T. Kanstad, T.A. Hammer, O. Bjøntegaard, E.J. Sellevold, Mechanical properties of young concrete: Part I: experimental results related to test methods and temperature effects, Mater. Struct. 36 (4) (2003) 218–225, https://doi.org/10.1007/BF02479614.

[75] D.J. Shen, C. Liu, M. Wang, J.C. Kang, M. Li, Effect of polyvinyl alcohol fiber on the cracking risk of high strength concrete under uniaxial restrained condition at early age, Construct. Build. Mater. 300 (2021), 124206, https://doi.org/10.1016/j.conbuildmat.2021.124206.
[76] H. Hedlund, Doctoral Thesis, in: Hardening Concrete: Measurments and Evaluation of Non-elastic Deformation and Associated Restraint Stresses, Lulea tekniska universitet, 2000.
[77] Eurocode 2, Design of Concrete Structures - Part 1-1: General Rules and Rules for Buildings, CEN, 2004.